한국윤활학회지(1995), 제 11 권 제 5 호
Journal of KSTLE(1995) Vol. 11, No. 5, pp.1~9

Spherical Particles Formation in Lubricated Sliding Contact -Micro-explosion due to the Thermally-activated Wear Process-

O.K. Kwon

Korea Institute of Science and Technology, Seoul, Korea

Abstract—The mechanism of various spherical particles formation from wide range of tribo-systems is suggested and deduced by the action of micro-explosion on the basis of the thermally-activated wear theory, in which the flash temperature at contact could be reached clearly upto the material molten temperature due to the secondary activation energy from the exothermic reactions involving lubricant thermo-decomposition, metals oxidation, hydrogen reactions and other possible complex thermo-reactions at the contacts. Various shapes of spherical particles generated from the tribo-system can be explained by the toroidal action of micro-explosion accompanied with the complex thermo-chemical reactions at the contact surfaces or sub-surfaces.

1. Introduction

Since the method of ferrography was developed to collect ferrous wear particles from the oil samples and to deposit them on the glass substrate [1], many researchers have reported on the observation of unusual wear particles, namely spherical particles of various morphologies, such as smooth-surfaced [2.3] or rough-surfaced [4-6] spheroids and hollow spherical particles [7-9], and also suggested of possible hypothesis to form such the shapes [9-14].

It is convenient that, spherical particles from the various tribo-systems could be classified into two major categories according to their morphology and size, namely smooth or rough-surfaced dense spheroids (Type I sphere) whose size is generally less than 10 μm and the hollow or ruptured-surface hollow spherical particles whose size are generally greater than 10 μm upto 150 μm (Type II sphere) [15].

For the observation of true particles or spheres generated from the original sources, it is crucially important to use a proper technique or apparatus to collect them on the substrate. In case of ferrography, it is very clear that the ferrography showed serious deleterious effect on the original wear particles into the smaller sized particles regrinded during the ferrogram preparation due to the pressurized squeezing action by the peristaltic pump [16]. This reason might lead many researchers to loose an opportunity to find bigger sized spherical particles upto 150 μm in many study cases.

To avoid the secondary re-grinding effect on wear particles, author and his colleague invented and introduced a new technique of the Rotary Particle Depositor (RPD). With the aid of RPD, many unusual particles and bigger sized spherical particles could be observed easily in many tribo-systems, which could hardly be observed before [17]. Hence, the RPD method could provide important information on the evaluation of the wear mechanism occurred in tribo-system through the originally formed wear particles.

The aim of the present work is to elucidate the possible formation mechanism of various spherical wear particles, especially generated in lubricated contact system on the basis of the thermally-activated wear theory.

2. Thermally-activated Wear Mechanism

This theory was developed as one of predominant wear mechanisms occurred in lubricated, concentrated sliding contact condition [18,19]. Primarily, the thermally-activated wear theory could provide a theoretical background of an additional thermal energy input (secondary activation energy) to the sliding contact system rather than a simple physical energy input, frictional energy input (primarily activation energy).

Experimental work was carried out by Four-Ball Wear Test machine.

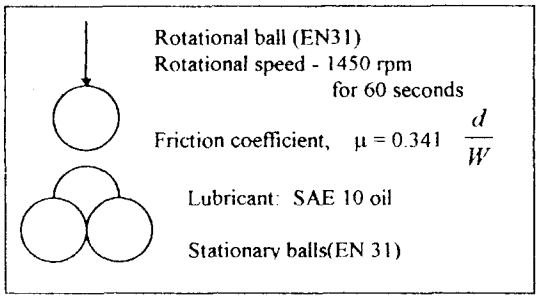

Fig. 1. Configuration of four-ball test system.

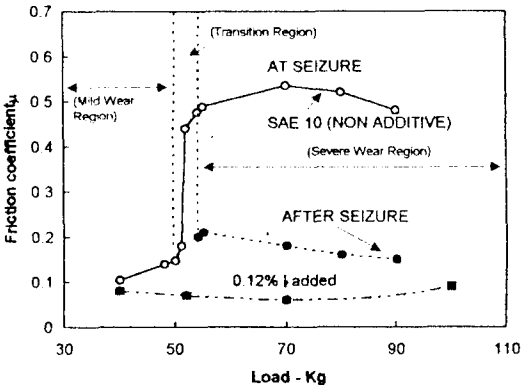

Fig. 2. Friction coefficient vs applied load.

In general, the four-ball machine provides very accurate repeatability in the test results and so many researchers use this machine to obtain reliable data in the study of wear and friction.

Fig. 2 shows a characteristic change in friction coefficient with the different wear mode changes. In Fig. 2, the bottom dot-line is the friction coefficient change with the sample oil added 0.12% I_2. In this experimental work, I_2 is used as a hydrogen scavenger to eliminate labile hydrogen atoms generated from the thermal decomposition of hydrocarbon at the frictional contact zone, in which the hydrogen atoms induce mainly complex thermo-chemical, metallurgical and exothermic reactions, resulting to the additional energy input (secondary activation energy) to the systems.

Fig. 3 shows the flash temperature (calculated from the results of friction coefficient in Fig. 2 by using Fein's modified Blok formula) change which indicates that the temperature rises dramatically in the transition wear period when seizure occurs, and continues to rise with load, becoming asymptotic to

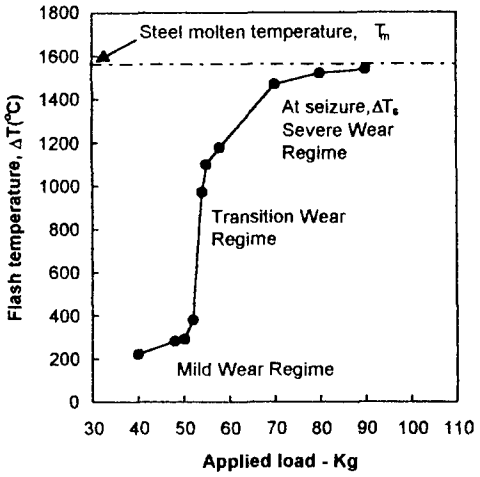

Fig. 3. Flash temperature vs applied load.

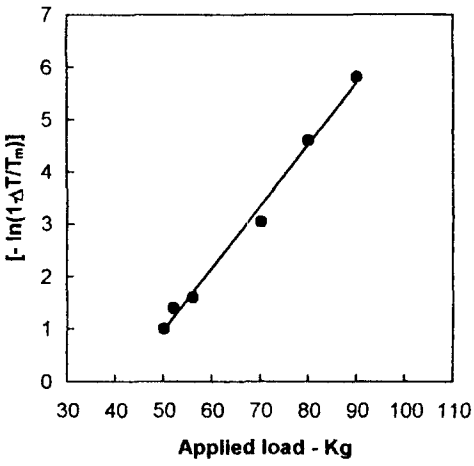

Fig. 4. Linear plotting of flash temp. against load.

the melting point of the steel (≅1570°C).

In Fig. 4, the plotting of the flash temperature (Δ T) relative to T_m, the molten steel temperature, on a logarithmic basis shows a good linear relationship with applied load for the seizure condition in the contact.

Much of the evidence obtained in this investigation from the micro-hardness measurements, sub-surface investigation by etching, and RPD analysis of wear particles, indicates the possibility of hydrocarbon reactions having occurred. Thermal decomposition of hydrocarbon lubricant generates products of atomic hydrogen and carbon. The former causes metal embrittlement, and the latter, when

diffused into a metal surface, increases the hardness. Most of reactions accompanying with atomic hydrogen and carbon are known as the exothermic reactions, which could provide a basic concept of the secondary activation energy input in thermal activated wear behavior.

2-1. The Basic Equation Governing Thermally-activated Wear Theory

The basic equation is driven from the first law of thermodynamics. Hence, the total activation energy (E) at a finite distance from the surface where the lubricant has penetrated is given by

$$E = Q - W \tag{1}$$

Where **Q** is total thermal energy supplied from external source, and **W** is work done to the surroundings.

The total thermal energy from an external source will arise mainly from frictional and compressive heat generation in the contact. The work done will include the effects of heat dissipation and initiation of thermal reactions of the hydrocarbons.

If it is assumed that most of the thermal energy involved in doing work is exerted to initiate the thermal reactions of hydrocarbons, the work function will be

$$W = -Q' + W' \tag{2}$$

Where **Q′** is the secondary thermal energy by exothermic reactions and **W′** is the resulting (net) work done to the surroundings, respectively.

Then equation (1) becomes as follow,

$$E = (Q + Q') - W' \tag{3}$$

The resulting net work done, **W′** includes the effects of metallographic phase transformation, crack initiation and propagation, the temperature rise of the outer-surface and sub-surface layers, and the possible consequential chemical and metallurgical reactions involved in the process.

It is evident that the time rate of change of the activation energy, **E** will be governed by the external mechanical and physical factors, viz., the combined effect of shearing and compressive stresses (**G**), the lubricant properties (μ), material properties (**M**), and environmental factor (ε). Hence,

$$\frac{dE}{dt} = f(G, \mu, M, \varepsilon) \tag{4}$$

For a sliding contact system in which the effect of lubricant factor (μ) and the environmental factor (ε) is neglected, dE/dt will be governed only by the stress factor (**G**) and the material properties (**M**), i.e., Eq. (4) becomes as,

$$\frac{dE}{dt} = f(G, M) \tag{5}$$

and from Eq.(3), the secondary thermal activation energy, **Q′**, will be zero. Hence,

$$\begin{aligned} E &= Q - W' \\ &= Q - W \end{aligned} \tag{6}$$

It is clear from Eq. (5) and Eq. (6) that the Eq.(5) implies a pure dry sliding system whereby no chemical reaction is involved. Hence, the total activation energy generated in the system could be determined only by two factors: the combined stress factor (**G**) and the material properties (**M**). The resulting wear behavior in this system will be determined by the magnitude of the total activation energy generated mainly from the sum of frictional and compressive heat, and the metal properties (**M**) is related to the thermal conductivity, metallographic characteristics, wear and frictional properties, bonding energy, and specific heat capacity, etc. In dry sliding, **Q** is sufficient for the temperature of the material to reach its melting point and then, welding will occur.

For lubricated situations, Eqs. (3) and (4) represent a more complex theoretical situation. Nonetheless, in most mixed and boundary lubricated conditions of operation, the resulting friction and wear behavior will be characterized by the total level of thermal energy, (**Q** + **Q′**), and the material properties (**M**), in which it is expected that (Q + Q′) will always be higher than **Q**, that is,

$$(Q + Q') > Q \tag{7}$$

It is also expected that W′ in Eq. (3), in terms of wear severity, will be increased by increasing the amount of (**Q** + **Q′**).

If we assume that the total thermal activation energy, (**Q** + **Q′**), is related directly to the sliding contact surfaces, then, it should be possible to determine the amount of **Q′** relative to **Q**.

To determine these quantities, it is necessary to introduce an effective hydrogen scavenger which can eliminate hydrogen effects and thus prevent any exothermic reactions occurring, or cause diffusion of

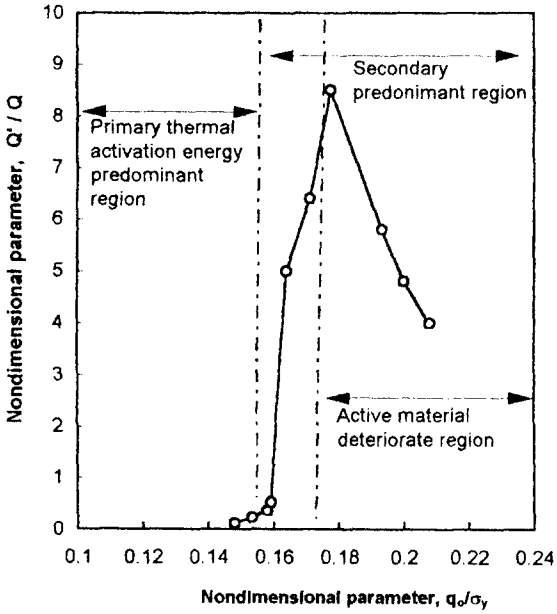

Fig. 5. Nondimensional parameters, Q′/Q vs q_o/σ_y.

hydrogen into the substrate. By comparing the results obtained in this manner with those obtained in the present work, it should be possible to determine the contribution of the secondary thermal activation energy to the wear controlling mechanism and subsequent wear behavior in the lubricated sliding contact.

In Fig. 5, the non-dimensional parameter, q_o/σ_y is arbitrarily introduced for convenience, rather than applied loads,where q_o is max. hertzian contact pressure [MN/m^2] and σ_y is yield stress of EN 31 [MN/m^2]. The non-dimensional ratio of secondary thermal activation energy to primary thermal activation energy, Q′/Q can be derived from the experimental results of flash temperature as,

$$\frac{(Q+Q')-Q}{Q} = \frac{Q'}{Q} \tag{8}$$

To establish Eq.(8), it is necessary to introduce an assumption that, in lubricated concentrated sliding contact (typically the four-ball scuffing condition), a combined stress effect generates frictional heat, followed by thermal energy cumulated very near the sub-surface and causing initiation of the secondary thermal activation energy. This additional thermal activation energy superimposes a further increase in sliding surface temperature, and the consequential effect is to increase the friction coefficient, due to the

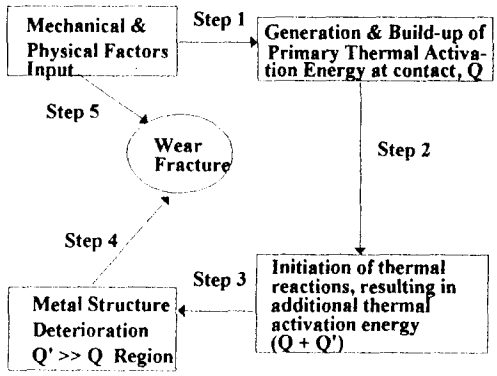

Fig. 6. Progressive diagram of thermally-activated wear behavior.

increased surface energy of the metal at the junctions [20].

From Fig. 5, it is evident that in the smooth sliding region (i.e. q_o/σ_y<0.16), the primary thermal activation energy due to mechanical frictional heat clearly dominates the secondary thermal activation energy. On the other hand, in the transition region, the relative amount of the secondary thermal activation energy increases abruptly, and increases further in the severe wear region to as much as eight times the primary thermal activation energy at 0.18 of q_o/σ_y. After this point, the ratio of Q′/Q shows a decrease with increasing load. The decrease of Q′/Q is considered to arise as a consequence of the secondary thermal energy being used to cause very active wear fracture of material in this stage. The active and severe wear fracturing behavior occurring in the region has been well identified by various experimental results [19].

In summary, the thermally-activated wear mechanism can depicted as the following diagram in five stage wear progresses.

3. Observation and Discussion

Many previous workers suggested and elucidated various mechanisms of formation of type I spherical particles generated from either drying contact or lubricated contact systems. Nevertheless, it is in fact that any comprehensive work or mechanism which provides generally an acceptable process of type II hollow spherical particle formation, hasn't been suggested yet. Therefore, in this work, the observations and discussions are concentrated mainly on the type

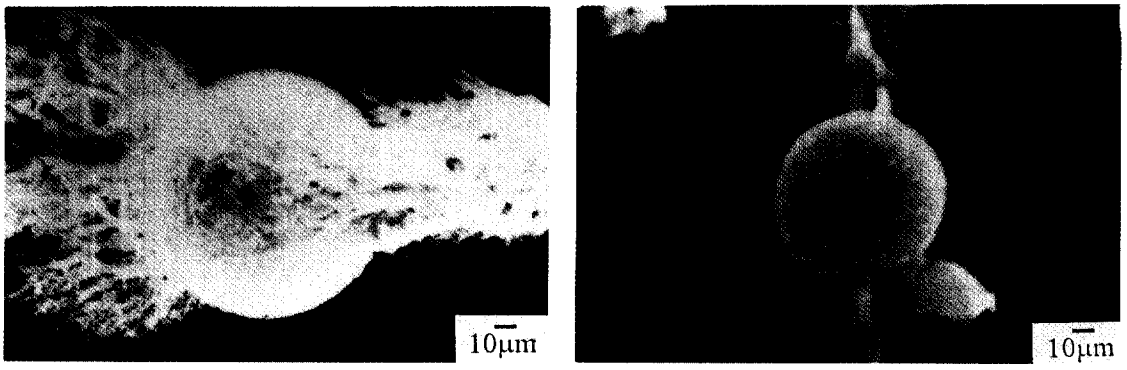

(a) (b)

Fig. 7. (a) Hollow spherical particle with eruptive holes on the surface, deposited with numerous number of ferrous dusty wear debris. (b) Type II sphere with dentrite-like surface morphology in same magnification of (a).

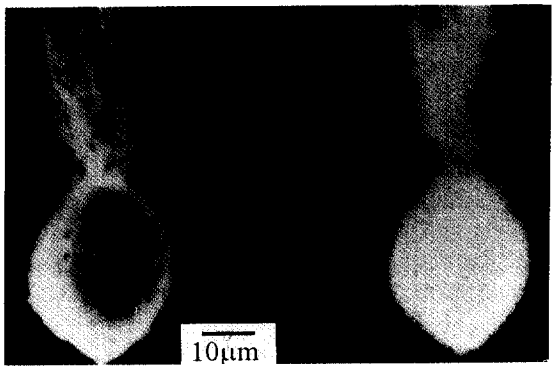

Fig. 8. Hollow spherical particle and its EDX image of Fe.

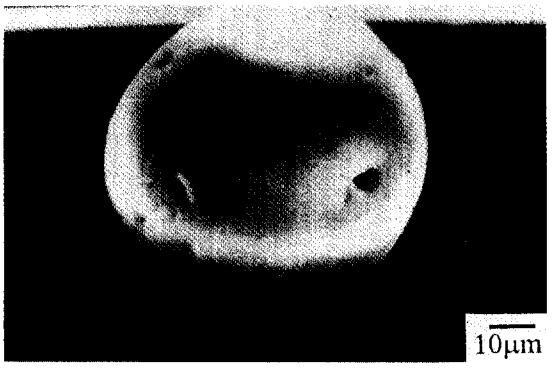

Fig. 9. Smooth surface hollow sphere from the transition wear region.

II spherical particles and also unusual particles which are possibly formed in the condition of thermal wear process.

Both particles in Fig. 7 (a) and (b) were collected from the oil samples tested at post transition region ($>q_o/\sigma_y=0.18$ in Fig. 5), e.g. severe wear region on Four-ball test. In Fig. 7, the most significant fact is the size of the hollow spherical particle which shows its size more than 100 μm. In this work, all the depositions of particles on the slides were prepared by RPD (Rotary Particle Depositor). It is very clear that the original size and morphology of the wear particles generated inherently could be possible to sustain in deposition by using RPD. Otherwise, by using ferrography, the deposition of wear particles is modified in size and morphology and leads mis-interpretation of the wear behaviour occurred. Fig. 8 also shows a typical hollow sphere with many surface spouting holes. A cuttle-fish like tail is a cluster of small normal wear particles deposited together. It is interesting that the surface morphology of Fig. 8 sphere is rather smooth than that of Fig. 7. The hollow spherical particle in Fig. 8 was generated in the condition of transition wear region. In general, it is in evidence that the hollow spherical particles generated in the transition region were comparatively smaller in size and showed smoother surface texture, comparing with those of the post transition.

Fig. 9 shows a typical spherical particle generated in the transition wear region, whose surface morphology is very smooth as-like ground.

Fig. 10 shows a numerous type II spherical particles deposited together with normal wear particles.

Fig. 10. Small size type II spheres. Some sphere shows eruptive hole on its surface.

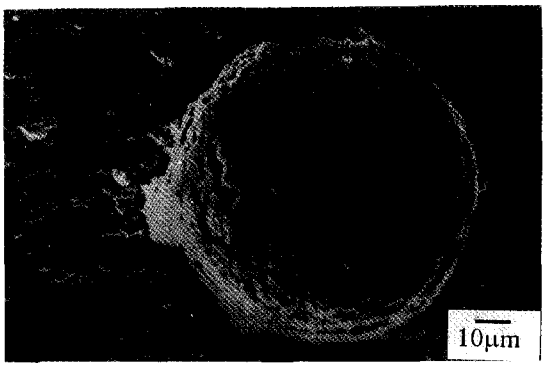

Fig. 11. Rolled-up sphere formed by snow-ball action.

Those spherical particles in Fig. 10 were generated from the post transition region, but their size is far smaller than previous Figs. 7 and 9. In general, the size of spherical particles also increased with the severity. It is not difficult to find the hollow spheres with their diameters over 100 μm in transition and also post transition wear region. An interesting finding from the results was that larger spheres (say, over 50 μm in diameter) were generally hollow and exhibited clear evidence of severe thermal experience on their inside or outer surface morphology. It is obvious that the reduced opportunity to observe the larger hollow spheres by previous workers, might be due to the crushing action on wear debris of the conventional ferrograph (16).

Fig. 11 shows a typical snow-ball like rolled-up spherial particle. The surface morphology suggests that many small size wear particles coagulated together by action of rolling up motion. In practice, the formation of rolled-up spherical particle could be possible only when the small wear particles were subjected to be molten state and the rolling action or strong toroidal action to coagulate each others be existed.

Apart from a comprehensive mechanism of formation of hollow and rolled-up particles, it is worthwhile to consider the possibility that the formation of microspheres is mainly due to local high temperature causing melting of the metal at contacts. In dry contact, the surface contact temperature could reach easily to the metal melting temperature, purely by frictional heat. However, it has not yet been possible to calculate or measure the actual contact temperature in lubricated contact situations. The contact temperature calculated on the basis of existing theoretical formulae is not enough to explain many phenomena of thermal behaviour known to occur. This problem may be consequent from the fact that the existing equations are purely concerned with the physical terms involved in solid contacts, but not with chemical energy terms arising from the accompanying complex chemical reactions between lubricants and solids at contacts. In this respect, this work provides a basic concept of total activation energy of thermal behaviour in lubricated situation. In addition, it is quite natural that the thermally-activated wear process postulates to accompany momentary high gaseous pressure and temperature at contact surface or sub-surface, which could provide a possible explanation of formation of various shapes of spherical partcles.

According to the results, it is evident that the more vigorous gaseous toroidal action could occur in the transition region than the post transition, caused to smoother surface feature shown in Fig. 9. That is, in Fig. 5, the most smooth-surface hollow spheres were generated from the range of $\mathbf{Q/Q'>5}$ and $q_o/\sigma_y \approx 0.17$-$0.18$. It suggests that the most severe inhomogeneous action involving gaseous thermal and chemical reactions might be occurred simultaneously within the above range on Four-ball contact system.

Fig. 12 shows an interior surface morphology of a hollow sphere. A quarter part of sphere was collected from the oil sample tested in post transition region. Its diameter is measured in SEM as big as 150 μm. The pebbled and dendrite-like interior structure also suggests a clear evidence of highly thermal

experience, viz., quick quenched after molten state of internal surface.

Fig. 13 shows a pre-matured type II spherical particle. This particle also was generated from the post transition region. The surface morphology is exactly the same as other hollow spherical particles seen in Fig. 7. The shape in Fig. 13 is considered to form at the intermediate stage of the hollow spherical particle, and may provide an important information on the formation procedure of the hollow spherical particle. That is, the shape provides clearly that, during the puffed out action by any pressurized gas from the inside of the particle at the molten state, it was / quickly quenched and solidified without further sorrounding whirling or toroidal action.

Fig. 14 shows a cross-sectional feature of a type II hollow sphere. The size of inside void in Fig. 14 (a) might have a co-relationship with the thermal expansion coefficient or the rate of shrinkage of EN 31 from the molten. Fig. 14 (b) shows EDX image of Fe on the cross-sectional surface and also micro-analysis results confirmed the same composites of EN 31.

Fig. 15 and Fig. 16 show very interesting features of different types of spheroid particles, in which both samples were prepared from the oil sample tested in post transition region. In Fig. 15, a bunch of hollow spheres are deposited with severe wear particles. Some spheres show a clear picture of deflated spherical shell and also some remain as blistered spheroids. This picture also suggests that high thermal environment of material molten state and vigorous gaseous action could generate many blisters at the contact surface or sub-surface, simultaneously.

The picture of Fig. 16 shows a cluster of solid spheriods. The general view of Fig. 16 is very interesting in relation to study the mechanism of formation of the spheroids. Some spheroids show a very exact feature of replicated shape against their neighbouring spheroids. These replicated shapes give a profound evidence of the formation of the

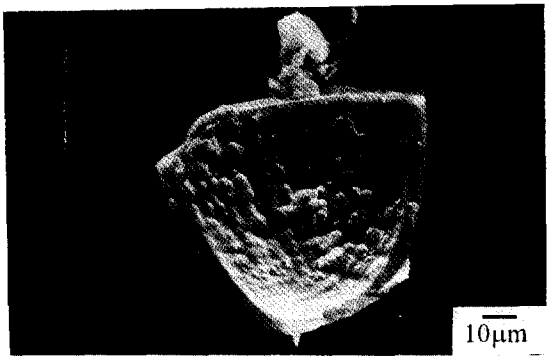

Fig. 12. Interior morphology of a quarter part of crushed hollow sphere.

Fig. 13. Pre-matured type II spherical particle.

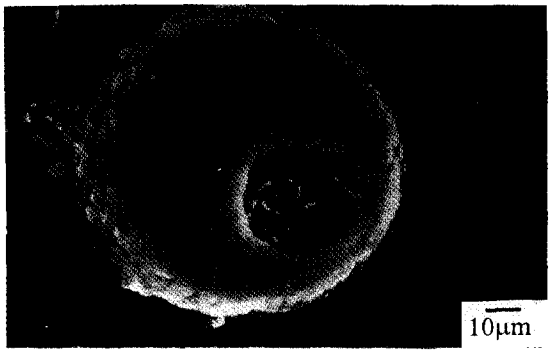

(a)

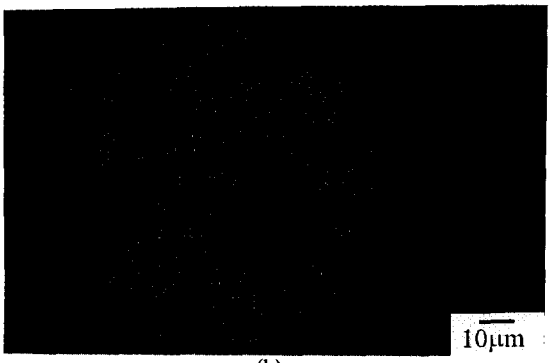

(b)

Fig. 14. (a) A cross-sectional feature of a type II sphere, polished and etched from mounted specimen. (b) EDX image of Fe on (a).

Fig. 15. A bunch of blistered hollow spheres.

Fig. 16. A cluster of type I solid spheroids.

Fig. 17. A glassy tubule with metallic dusts on its surface.

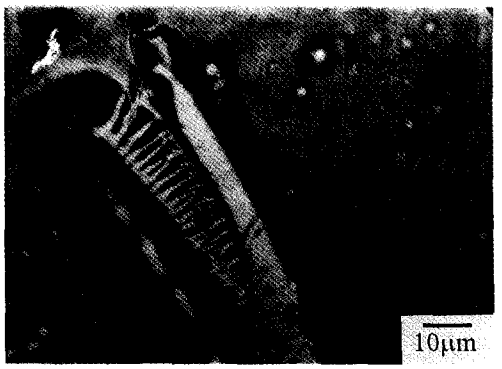

Fig. 18. A cylindrical shape of glassy tubule showing inside branchial structure (×400 optical).

cluster. Namely, various spheroid particles in the cluster in Fig. 16 might be formed by a sequential splashing action from the molten material source. During the sequential splashing action of the molten material, the above mentioned replicated shape of spheroids could be easily formed, when the molten splits collide against ready-formed spheroids, instantaneously.

Fig. 17 and 18 are unusual wear particles, a glassy tubule and a cylindrical, glassy tubule. These kinds of particles are not difficult to observe from the ferrograms with the samples testes in transition and post transition regions. It is interesting that the population of glassy tubules or cylindrical tubules increased abruptly at the point of maximum value of **Q′/Q**, that is, when the secondary activation energy becomes maximum, as seen in Fig. 5.

Fig. 17 shows a perfect shape of a piece of broken tubule and its surface is impregnated by many small metallic dust-like particles. The true mechanism of formation is not known yet, but it is supposed to form at the subsurface at the contact, due to the consequential interactions of metallurgical, mechanical, and complex thermo-chemical reactions. EDX analysis confirmed that the major element of the tubule was Si, with minor elements of Fe, Cr and carbon. It is unclear, where the major composite of silicon came from, thermally etched out from the EN31 or from the lubricants.

The analysis results of Fig. 18 also show similar to that of Fig. 17. But the shape seems to be formed under the rolling mechanism. The branchial feature of the inside structure may also impose a possibility that the internal part of the tubule was subjected to the flowing gas stream of extremely high temperature and pressure.

4. Conclusions

From the results of examination and discussion, it

could be concluded that the wear process in thermally-activated wear mechanism occurs sequentially in four separate steps, but closely-linked three stages, as summarised in Fig. 5 and Fig. 6. On this basis, the wear behaviour may be specified in terms of three different modes: Mode 1 is associated with primary thermal activation energy effects. Mode 2 relates to secondary thermal activation energy; and Mode 3 defines a region in which active material deterioration occurs due to the secondary thermal activation energy effects.

The secondary thermal activation energy is mainly caused and cumulated by the thermal reactions of hydrocarbons, subsequently followed to produce atomic hyrogens and carbons which lead to the strong exothermic reactions of oxide reduction by hydrogen, moleculising reacton of atomic hydrogen, graphitisation of carbons and carbide formation , etc. In Mode 2 and Mode 3, it is also possible to consider that, the condition of micro-explosion or micro-self-ignition at the subsurface or at the contact surface could be easily attained by the liquid-vapour mix. phases of hydrocarbons, air, metallic dust and high temperature and pressure.

In conclusion, it is proposed that severe toroidal turbulence action due to micro-explosion and vigorous thermal reactions at the subsurface or near subsurface of the contacts, accompanied by momentary high pressure and temperature which melt the surrounding metal dust or wear debris, provide the basic mechanism to produce the various spherical particles and unusual glassy tubules discussed previously, in lubricated concentrated contact processes.

References

1. W.W. Seifert and V.C. Westcott, "A method for the study of wear particles in lubricating oil," Wear, 21, 27-42 (1972).
2. D. Scott and G.H. Mills, Wear, 24, 235 (1973).
3. B. Loy and R. McCallum, Wear, 24, 219 (1973).
4. E. Broszeit and F. J. Hess, Wear, 17. 314 (1971).
5. A. V. Sreenath and N. Raman, Tribology, 55 (April 1976).
6. T.A. Dow and R.A. Burton, J. Lubr. Technology, 357 (July 1977).
7. A.W. Ruff, Wear, 42, 49-62 (1977).
8. M.H. Jones, Wear, 90, 75-88 (1983).
9. Jin Yuanshen and Wang Chengblao, Wear, 131, 315-328 (1989).
10. K. Hack and H. G. Feller, Z. Metallkd., 61, 394-400, German (1970).
11. H. Charney, "Fundamentals of interfacial slip damping," BS and MS Thesis in Mechanical Engineering, MIT USA, June 1970.
12. D. Scott and G.H. Mills, Wear, 16, 234-237 (1970).
13. I.F. Stowers and E. Rabinowicz, Appl. Phys. 43, 2485-2487 (1972).
14. Ernest Rabinowicz, Wear, 42, 149-156 (1977).
15. D.G. Jones, MSc Thesis, University College of Swansea (1980).
16. D.G. Jones, D.A. Vaughan and O.K. Kwon, Wear, Vol.90 No.1, 63-73 (1983).
17. O.K. kwon, "Application of Rotary-ferrography," Proceedings of '84 International conference of condition monitoring, 10-13th April, 1984, Swansea, UK.
18. F.T. Barwell, O.K.Kwon, B.J. Roylance, "Interaction of Chemical, Thermal and Mechanical Factors in the Lubrication of Machine Elements", 3rd Int Tribology Congress, Sept, Euro trib., Warzawa, 1981.
19. O.K. Kwon, Ph.D. Thesis, University of Wales, Swansea, 1981.
20. E. Rabinowicz, "Friction and Wear of Materials," 1965, John Wiley & sons.